

EUROPEAN ORGANIZATION FOR NUCLEAR RESEARCH

European Laboratory for Particle Physics

CERN - SL DIVISION

CERN SL/95-16 (EA)
NA48 Note 1995-13

**A NOVEL APPLICATION OF BENT CRYSTAL CHANNELING
TO THE PRODUCTION OF SIMULTANEOUS PARTICLE BEAMS**

N. Doble, L. Gatignon and P. Grafström

Abstract

Channeling of a 450 GeV/c proton beam through a bent Silicon crystal has found a novel application to the production of simultaneous particle beams. A pair of simultaneous, nearly-collinear beams of long- and short-lived neutral kaons has thereby been derived. These beams form an integral part of an experiment, NA48, at CERN, designed to measure the CP-violation parameter ϵ'/ϵ with high precision.

To be submitted to Nucl. Instr. and Meth.

and

to be presented at the Workshop on "Channeling and other Coherent Crystal Effects
at Relativistic Energy",
Aarhus, Denmark, July 10-14, 1995

Geneva, Switzerland
March, 1995

CONTENTS

	<u>Page</u>
1. INTRODUCTION	1
2. BEAM LAYOUT	2
3. THEORY OF THE BENT CRYSTAL APPLICATION	3
4. MECHANICAL CONSTRUCTION AND CONTROL	5
5. TUNING AND RESULTS	6
5.1 Beam Tuning	6
5.2 Crystal Tuning	7
5.3 Transmission	9
5.4 Second Crystal	10
6. CONCLUSIONS	10
7. ACKNOWLEDGEMENTS	11
8. REFERENCES	12
TABLES	14
FIGURES CAPTIONS	17
FIGURES	19

1. INTRODUCTION

A pair of simultaneous, nearly-collinear beams of long- and short-lived neutral kaons forms an integral part of an experiment, NA48, at the CERN Super-Proton-Synchrotron (SPS), designed to measure the CP-violation parameter ε'/ε with high precision [1]. The principle of the measurement depends on comparing the relative decay rates into two neutral and into two charged pions of long- and short-lived neutral kaons (K_L and K_S , respectively)¹. To reduce systematic differences, the two decay modes from each of the two kaon beams are detected simultaneously. The K_L and K_S beams are derived from protons striking two separate targets, spaced 120 m apart longitudinally. The two kaon beams enter a common decay volume, which leads to a series of detectors specialised in recording the charged pions and the photons resulting from decay of the neutral pions. The layout of the beams and detectors is described in Section 2.

In this context, the phenomenon of channeling in a bent crystal finds a novel application. When charged particles pass through a mono-crystal at an angle close to a crystallographic direction (axis or plane), the coherent scattering on the lattice nuclei forces the particles to follow the lattice direction. This remains true, though with somewhat increased losses, if the crystal is bent mechanically. Therefore a bent crystal can be used in place of a magnet to deflect a beam of charged particles. The phenomenon of channeling has been discussed extensively in the literature [2,3,4,5] and has recently been reviewed in lecture form [6], giving a complete set of references and a bibliography. Experimental studies, especially on planar channeling and bending, have been performed at various accelerators [7,8,9,10], notably with a beam of 450 GeV/c protons from the CERN SPS incident on a Silicon crystal [11,12,13].

In principle, a bent crystal lends itself ideally as a beam splitter for the 450 GeV/c primary proton beam used to produce the two kaon beams. The part of the beam used to produce the K_S is required to have a greatly reduced flux, within a well-defined emittance, and should be selectively deflected away from the accompanying background of charged particles.

Section 3 discusses the theory of a novel application of this technique to derive the two beams. The mechanical construction and control of the bending

¹ The parameter of interest is related to the measured double ratio of the $K^0 \rightarrow \pi\pi$ decay rates:

$$\varepsilon'/\varepsilon = \frac{1}{6} \left[1 - \frac{\Gamma(K_L^0 \rightarrow \pi^0\pi^0 \rightarrow 4\gamma)}{\Gamma(K_L^0 \rightarrow \pi^+\pi^-)} \bigg/ \frac{\Gamma(K_S^0 \rightarrow \pi^0\pi^0 \rightarrow 4\gamma)}{\Gamma(K_S^0 \rightarrow \pi^+\pi^-)} \right].$$

device and goniometer are described in Section 4. The tuning procedure and results obtained in the course of a two month period of beam studies in 1994 are presented in Section 5 and the main conclusions are drawn in Section 6.

2. BEAM LAYOUT

The basic layout for the production of the two simultaneous, K_L and K_S beams is shown schematically, in vertical section, in Figure 1.

Nominally, a flux of $1.5 \cdot 10^{12}$ 450 GeV/c primary protons per SPS pulse are focussed onto a 2 mm diameter, 400 mm long Beryllium target, at a downward angle of 2.4 mrad, to produce the neutral, ' K_L ' beam, which points horizontally towards the detectors. The target station is followed by a dipole magnet to sweep away charged particles. This magnet deflects the remaining primary protons ($\sim 6 \cdot 10^{11}$ per pulse) further downwards by 7.2 mrad, so that, at a distance of 10.95 m from the target, they are centred 72 mm below the K_L beam axis. At this point the crystal is installed, with the purpose of selecting and deflecting a wanted, small fraction ($\sim 5 \cdot 10^{-5}$, corresponding to $\sim 3 \cdot 10^7$ per pulse) of these protons upwards by 9.6 mrad, so they can pass horizontally through a 2.4 mm diameter aperture in the subsequent beam dump/collimator. The majority of the protons, not channeled by the crystal or interacting in its holder, continue undeviated and are absorbed in the tungsten-alloy inserts of the dump/collimator at a (downward) angle and displacement of 9.6 mrad and ~ 14 mm, respectively, from the wanted beam of protons.

Downstream of the dump, further dipole magnets deflect the wanted protons back onto the K_L axis, allowing them first to be recorded by a system of 'tagging' counters with high space- and time-resolution [14]. In passing along the K_L beam axis, the protons are refocussed by a series of four quadrupole magnets to a focal point 109 m downstream of the crystal. Before reaching this focus, they are again deviated away by dipole magnets to reach a point 72 mm above the K_L beam. Here a second target (of similar dimensions to the K_L target) is located to serve as source for the production of the ' K_S ' beam. This beam is arranged to have a production angle of 4.2 mrad, in order to render the momentum spectrum of the detected K_S decays as similar as possible to that of the K_L over the chosen range (70 - 170 GeV/c). The K_S target is also followed by a dipole sweeping magnet, packed with tungsten-alloy inserts (in which the protons not interacting in the target are finally absorbed) and by a collimator defining a downward direction of 0.6 mrad and ending 6.0 m after the K_S target. From here on, the K_S beam and the ongoing K_L beam emerge into a common decay volume, through which they pass 'simultaneously and nearly-collinearly', converging towards the principal detectors of the experiment, 114 m further downstream.

The proton and neutral kaon beams are transported in vacuum, over a length of ~ 250 m from the exit of the K_L target station and finally passing through a central hole in the detectors of the experiment. The vacuum is only interrupted by thin windows separated by a 4.6 m long section of air at the location of the crystal and dump/collimator and by a pocket, which houses the tagging counters on the proton beam used for the K_S (as indicated in Figure 1).

3. THEORY OF THE BENT CRYSTAL APPLICATION

Generally, the deflection of protons by planar channeling through a bent crystal has been studied with a beam of small divergence, incident perpendicularly onto one end and exiting from the other end of the crystal, which has been curved about an axis perpendicular to the beam direction. In that case the emittance of the deflected beam is only restricted in the plane of deflection, by the thickness of the crystal and by the critical angle for planar channeling ($\sim \pm 7$ μ rad for the 110 planes of Si at 450 GeV/c). With a highly parallel beam, transmission efficiencies of $\sim 10^{-1}$ for deflections of ~ 10 mrad have been observed [11,12,13].

In the present application, a transmission efficiency of only $< 10^{-4}$ is required. The beam diverges onto the crystal from a focal point (at the K_L target) 10.95 m upstream. In order to transport the deflected beam cleanly via the tagging counters onto the K_S target, it is important to limit its emittance in both the horizontal and the vertical (bend) plane. Moreover, a robust method is sought to fine-tune the angle of deflection of the protons through the crystal, without being sensitive to heating induced by the incident beam in a region intended to be exposed to $\sim 10^{12}$ protons/cm² per pulse (of 2.4 s duration every 14.4 s) and an integrated fluence per year of up to $\sim 10^{18}$ protons/cm² ².

These considerations led to the adoption of a design for the crystal mounting which is described in detail in the next Section. The guiding principle is to use a crystal which is bent through a fixed total angle (θ_0) greater than that required for the beam. The crystal is then rotated through an azimuthal angle $\pm \phi$ (about a vertical axis), such that the beam impinges on one side edge, traverses the crystal diagonally and exits from the opposite edge, as shown schematically in Figure 2. The fractional length of the bent crystal traversed and hence the angle of (vertical) deflection, θ , of the beam is then governed by the angle of rotation, ϕ , which can be adjusted smoothly.

² A recent review of radiation damage studies suggests that deterioration of the channeling properties of Si crystals exposed to high-energy protons may set in only at an integral fluence $> 10^{20}$ protons/cm² [15].

Furthermore, the vertical inclination (y') of the planes encountered along the crystal edge depends on the transverse (horizontal) point of incidence of the beam (x co-ordinate), such that the crystal channels and deflects protons with a well-defined ratio $\Delta y'/\Delta x$. This introduces a coupling between the angle in the vertical plane for channeling to occur and the horizontal position co-ordinate at the crystal, which in turn is correlated to the horizontal divergence (x') of the beam. The result is an outgoing beam, which is defined in BOTH planes.

The co-ordinate system and geometry of the bent Silicon crystal³ are defined in Figure 2. The principal geometrical parameters, the formulae from which they are derived and their chosen design values are listed in Table I. The essential properties related to channeling in the Silicon crystal are summarised in Table II.

Figure 3 illustrates the propagation of the typical proton beam phase-space in the vertical (y, y') and horizontal (x, x') planes - from the focus at the K_L TARGET to the CRYSTAL, and thence selected by the crystal⁴ and transmitted downstream to the tagging counters (TAGGER). The proton beam transport has also been simulated using the Monte Carlo programme 'DECAY TURTLE' [16]. This was modified to include the cuts on the beam phase-space, in both position and angle co-ordinates, due to the crystal acceptance for channeling. Comparisons of the predicted and measured transmission and profiles of the beam onto the tagging counters are presented in Sections 5.3 and 5.4, respectively.

³ The choice of crystal material to be Silicon was based on the relative ease of growing a large mono-crystalline ingot, from which a series of similar crystals could be cut parallel to the uniformly-spaced (110) planes. Moreover, we could profit from the experimental data already obtained with similar crystals [11,12]. For the purpose of minimising interactions of protons in the crystal, a material of relatively low atomic weight and density is advantageous.

⁴ The fraction, f , of the beam emittance falling within the crystal acceptance for channeling may be estimated from Figure 3 to be :

$$f \approx \frac{8 t \cdot \psi \cdot \Delta x / \Delta y'}{\pi^2 x'_o \cdot y'_o \cdot z^2} \approx 7 \cdot 10^{-4} ,$$

where $t = 1.5$ mm, $\Delta x / \Delta y' = 1.64$ mm/mrad (Table I), $\psi \approx 0.007$ mrad (Table II), $x'_o \approx 0.8$ mrad, $y'_o \approx 0.2$ mrad are the horizontal, vertical (half-width) divergences of the beam from the focus at the K_L target and $z = 10.95$ m is the longitudinal distance of the crystal from the focus.

4. MECHANICAL CONSTRUCTION AND CONTROL

The bending device, on which the crystal is mounted, is shown in Figure 4. Its design is based on the following considerations :

- i) The bending device is constructed from a solid block of aluminium, precisely machined to have a cylindrical face of the wanted radius of curvature (3.00 m) for the crystal. Aluminium is chosen as a relatively low-density material, of mechanical and thermal properties close to those of the silicon crystal itself and which lends itself to precise machining. Moreover, its high thermal conductivity serves to disperse the local heating produced by the incident beam in the crystal and in the adjacent part of the block⁵ .
- ii) The crystal is pressed against the curved surface of this block by two cylindrical rollers, so as to avoid transmitting any tangential component of force to the crystal. The rollers are situated close to each end, touching only parts of the crystal which are in principle not traversed by the beam.
- iii) The force applied to each roller (~ 2 kg) is designed to be only moderately greater than that required to bend the crystal (elastically) into contact with the cylindrical face of the aluminium block⁶. The force is adjusted by means of screws fitted with spring washers, which transmit a known force when compressed⁷.

The crystal holder constitutes a robust, radiation-hard and easily-exchangeable unit, which is pinned and screwed onto a goniometer, shown in Figure 5. This is equipped with computer-controlled, motorised movements⁸ and corresponding position-sensitive captors, which allow displacements to be

⁵ For the nominal flux of $\sim 6 \cdot 10^{11}$ protons per pulse striking the crystal and its holder every 14.4 s, the increase in temperature of the aluminium block is estimated to be $\sim 10^{-2}^{\circ}\text{C}$ per pulse to reach an equilibrium increase (with cooling by natural convection and radiation) of $\sim 3^{\circ}\text{C}$. The temperature can be monitored by a thermo-couple set into a hole in the block. During the present beam test at $\sim 1/5^{\text{th}}$ of nominal flux, no significant temperature increase was observed ($< 1^{\circ}\text{C}$).

⁶ Earlier tests showed the destructive action of applying excessive localised pressure to the part of the crystal used for proton channeling [17].

⁷ The curvature of the crystal could be checked after mounting, by recording, as a function of position, the change in angle of a laser beam reflected off its (polished) surface. Over the central region of interest, it was found to agree with the nominal radius of curvature to within $\sim 5\%$.

⁸ The motorised goniometer used was manufactured by OWIS GmbH, Staufen, Germany. A radiation-resistant execution is being equipped with motors from PHYTRON-Elektronik GmbH, Gröbenzell, Germany, rated to withstand an integrated dose of 10^8 Gray, (~ 100 times the dose expected in the course of the experiment).

made and controlled in four co-ordinates, with the following ranges and minimum step sizes :

- i) Horizontal, transverse displacement, x :
-141 mm (out of beam) $< x < +11$ mm, $\Delta x = 0.03$ mm;
- ii) Vertical displacement, y :
-5 mm $< y < +9$ mm, $\Delta y = 0.01$ mm;
- iii) Horizontal, azimuthal angle (about a vertical axis), φ :
-35° $< \varphi < +35$ ° $\Delta\varphi = 0.01$ °;
- iv) Vertical angle of inclination (about a horizontal axis transverse to the crystal), α :
-160 mrad $< \alpha < +160$ mrad, $\Delta\alpha = 0.04$ mrad.

The whole goniometer ensemble is constructed from radiation-resistant components. It rests in turn on a massive, pre-aligned, plug-in base, onto which it is lowered and guided by means of a locally-controlled, rack-and-pinion lifting device. This allows the exchange of crystal holders or any intervention on the goniometer to be made with the ensemble raised to the top of the shielding blocks, which surround the beam.

5. TUNING AND RESULTS

5.1 Beam Tuning

Before the crystal co-ordinates can be tuned, the primary proton beam, previously steered in position and focussed onto the K_L production target, has first to be steered in direction. This was performed by defining a pencil beam, with collimators upstream of the K_L target, which followed the central trajectory of the full beam and had a flux reduced to $\sim 10^7$ protons per pulse, (comparable to the flux required to produce the K_S beam). By making calculated changes to the strengths of the dipole magnets : BENDs 1, 2 and 3 (Figure 1), this pencil beam was brought to follow a trajectory ("A" in Figure 1), which by-passed the crystal in the vertical plane. The (mobile) beam dump/collimator was also moved upwards by the calculated displacement. Upstream dipole magnets were then used to pivot the beam about the centre of the K_L target. It was steered in direction in both the horizontal and vertical planes, so as to maximise the relative flux passing through the aperture in the

beam dump/collimator and counted on a scintillation counter (TRIG), located at the downstream end of the K_L neutral beam line⁹.

The strengths of BENDs 1, 2 and 3 and the position of the beam dump/collimator were reset to follow the nominal beam trajectory ("C" in Figure 1). The full-emittance proton beam was then re-established, with its flux restricted to between 2 and $4 \cdot 10^{11}$ protons per pulse, so as not to saturate the beam counters used. This beam was used to tune the crystal.

5.2 Crystal Tuning

Starting from the nominally aligned settings (see Table III), an iterative search to find the optimum settings of the crystal goniometer positions and angles was then undertaken.

An example of this procedure is described and commented below and the results obtained are illustrated in the sequence of Figure 6 a) - e) :

- i) The channeling condition was sought by scanning the crystal vertical angle, α (in steps of $\Delta\alpha = 0.2$ mrad), and counting the flux of particles reaching the TRIG counter normalised to the flux of protons incident at the K_L target, (Figure 6 a)). The central setting, $\alpha = + 6.2$ mrad, was selected.
- ii) The vertical beam deflection angle (θ) was varied by scanning the crystal angle in the horizontal plane, φ (in steps of $\Delta\varphi = 0.2^\circ$, corresponding to $\Delta\theta = - 0.1$ mrad), (Figure 6 b)). The setting $\varphi = + 30.0^\circ$ was selected.

A tail in the distribution is seen towards low values of φ . It was interpreted as being due to protons leaving the edge of the crystal beyond the roller at its downstream end, where the crystal ceases to be curved against the holder (Figure 2). This observation, together with the off-set in α found with respect to 5.5 mrad (Table I), suggested that the horizontal position of the crystal should be displaced by :

$$\Delta x = + (6.2 - 5.5) \text{ mrad} \cdot R \sin \varphi \approx + 1 \text{ mm.}$$

- iii) The crystal was in fact displaced horizontally by + 2.0 mm (see below) and the vertical angle, α , was rescanned (Figure 6 c)). The full width of the distribution is given by the horizontal size of the beam at the crystal

⁹ For this and the subsequent exercises, the K_L beam was blocked at the beam dump/collimator and the refocussing quadrupoles and the downstream deflecting magnets of the proton transport to the K_S target were switched off.

($\delta x \approx 2.0$ mm) that can pass through the 2.4 mm diameter aperture in the following beam dump/collimator, via the relation :

$$\delta\alpha = 1/\cos \varphi \cdot |\Delta y'/\Delta x| \cdot \delta x \approx 1.4 \text{ mrad.}$$

The setting $\alpha = + 4.7$ mrad was selected.

- iv) The vertical position, y , was scanned (in steps of $\Delta y = 0.4$ mm), (Figure 6 d)). The full width of the distribution is given by the sum of the thickness of the crystal ($t = 1.5$ mm) and the height of the beam ($\delta y \approx 2.0$ mm) that can pass through the beam dump/collimator aperture :

$$t + \delta y \approx 3.5 \text{ mm.}$$

The central setting, $y = - 1.5$ mm was selected.

- v) The horizontal angle, φ , was then rescanned (Figure 6 e)). We note that the tail seen in Figure 6 b) has been suppressed, supporting the explanation given under point ii) above. The width of the distribution is given by the spread in vertical angle of the beam impinging on the crystal ($\delta y' \approx 0.23$ mrad), via the relation :

$$\delta\varphi = 2 |\Delta\varphi/\Delta\theta| \delta y' \approx 1.0^\circ,$$

as long as the corresponding variation in exit angle is accepted by the downstream passage leading to the TRIG counter.

A central setting, $\varphi = + 30.1^\circ$, was adopted.

- vi) With the settings thus obtained, the horizontal and vertical profiles of the transmitted proton beam were observed on a wire chamber, MWPC, located immediately in front of the TRIG counter (~ 243 m downstream of the crystal). These profiles are shown in Figure 7.

With the same crystal, a second, symmetrical solution is expected with an opposite horizontal rotation, $\varphi \sim -30^\circ$. The corresponding scans of α , y and φ are shown in Figure 8 a), b), c), respectively, yielding central settings :

$$\alpha = + 4.1 \text{ mrad, } y = - 1.3 \text{ mm, } \varphi = - 28.1^\circ.$$

The similarity of this value of α to that found under iii) above indicates that the horizontal position of the crystal had been well centred.

The two sets of settings obtained with this crystal are summarised in Table III.

5.3. Transmission

With either of the settings of the crystal found above, a transmission to the tagging counters (and thence to the TRIG counter) of $\sim 4 \cdot 10^{-5}$ of the protons incident onto the K_L target was recorded. This corresponds to $\sim 1.0 \cdot 10^{-4}$ of the protons leaving the target and impinging onto the crystal and its holder. Taking into account the phase-space of the incident beam and the crystal acceptance shown in Figure 3 and simulated by Monte Carlo calculation (see Footnote 4) to Section 3), it represents ~ 0.15 of those protons falling within the critical angle for channeling with respect to the crystal planes. The transmission found is thus in fair agreement with other measurements [11, 12, 13] and with theoretical expectation [5, 6], taking into account a crystal surface transmission, $S \approx 0.7$, and a transmission factor due to dechanneling through the bent crystal of $\eta \approx 0.2$ (see Table II).

As indicated in Section 2, the experiment nominally requires a fraction of $\sim 5 \cdot 10^{-5}$ of the protons leaving the K_L target to be transmitted and deflected via the tagger onto the K_S target.

The overall transmission can be varied (reduced) by increasing the horizontal extent of the beam incident onto the crystal. In fact, the beam optics leading to the K_L target had already been arranged to give a large (factor 3) magnification in horizontal divergence of the beam at the target, in order to limit this transmission. A further, convenient way to reduce the transmission was found in pivoting the whole beam in horizontal angle about the K_L target. This lowers the local intensity of protons striking the crystal over the small horizontal extent found to correspond to conditions for channeling.

With the crystal settings found for $\varphi = + 30.1^\circ$ (Table III), the relative flux of protons transmitted onto the tagger was recorded as a function of the current in a steering dipole magnet, located at a horizontal intermediate focus of the proton beam upstream of the K_L target. This scan is shown in Figure 9. The current in the magnet relates directly to the angle in the horizontal plane of the trajectory of the beam at the K_L target and hence to its displacement onto the crystal. Thus Figure 9 represents a horizontal profile of the beam, with the crystal transmission used to measure the relative intensity at each point. The transmitted flux was maximum for the setting P, for which the profiles of the beam obtained at the wire chamber, MWPC, are shown in Figure 10 a). It was demonstrated that the flux could be tuned (reduced) without affecting the beam

quality significantly¹⁰. The nominally required transmission was attained with setting Q, for which the corresponding beam profiles, shown in Figure 10b), have similar widths and centres to within, respectively, $\sim \pm 5\%$ and $\sim \pm 2\text{ mm}$ (corresponding to $< \pm 0.01\text{ mrad}$ variation in angle from the crystal).

5.4. Second Crystal

Towards the end of the beam studies, the crystal used for the above measurements was replaced by a second, similar crystal, mounted in its own holder. A similar tuning procedure was followed and the goniometer settings found are given in Table IV. The relative transmission observed was found to be comparable within $\sim \pm 10\%$ to that observed with the first crystal, as were the shapes and widths of the beam profiles. Those obtained with the crystal settings found for $\varphi = -27.5^\circ$ (Table IV) are shown in Figure 11.

With the same settings of the second crystal, furthermore, the profiles of the protons were recorded at the position where they have to be tagged. For this purpose, a scintillating-fibre hodoscope [18] was constructed and installed immediately preceding the TAGGER. The profiles obtained at this position are shown in Figure 12, for the nominal ratio of protons to the K_L and K_S targets. The shapes and widths of these profiles compare well with those derived from Figure 3 and from Monte Carlo simulation of the crystal acceptance, (see Section 3).

6. CONCLUSIONS

The principle of bent crystal channeling has been applied in a novel technique to produce simultaneous, nearly-collinear beams of long- and short-lived neutral kaons to the CP-violation experiment NA48.

The technique offers a unique combination of features, essential to that experiment :

- i) The flux of the transmitted beam is reduced by more than four orders of magnitude, without the deterioration of beam quality usually associated with the processes of attenuation and tight collimation.

¹⁰ It is important for the experiment that the ratio of K_S to K_L beam fluxes remains roughly constant during each pulse. This 'detuning' of the proton beam onto the crystal renders the K_S flux sensitive to time-variations in the angle of the primary beam extracted from the SPS. It is therefore planned to monitor the K_S and K_L beam fluxes in intervals of time and to use their ratio to adjust the current in the steering magnet via a feed-back loop.

- ii) The resulting beam automatically has a small, well-defined emittance in BOTH planes.
- iii) The wanted beam is selectively deflected in the desired direction, without cancelling the effect of the preceding sweeping magnet on all unwanted charged particles¹¹.

These features have been proved in the course of beam studies carried out in 1994. The principal results, presented in this report, bear out the basic capability of the bent crystal to meet the stringent beam requirements of this experiment.

7. ACKNOWLEDGEMENTS

It is a privilege to express our indebtedness to E. Uggerhøj of the University of Aarhus, Denmark, for introducing us to the field of crystal channeling and bending, which he has pioneered at CERN. He procured the mono-crystalline ingot of Silicon from TOPSIL A/S., Frederikssund, Denmark. From this, a series of ten crystals were cut and polished to the wanted orientation and dimensions by P. Keppler and colleagues of the Max-Planck-Institut für Metallforschung, Stuttgart, whom we wish to thank for their meticulous work.

We also profitted from the experience and advice of colleagues from the Aarhus, CERN, Strasbourg bent-crystal collaboration, especially S.P. Møller, K. Elsener and U. Mikkelsen. The detailed design of the crystal holder and the specification of the goniometer, as well as the overall organization of the beam installation, are due to M. Clément. Many parts were carefully constructed and the crystals mounted and measured by R. Allegrini. The motorization and electronics for the goniometer were integrated into the SPS computer control system by K.D. Lohmann and C. Beugnet, with application programmes written by G. Dubois and A. Bonifas.

The work was carried out in the framework of the NA48 collaboration (Cagliari, Cambridge, CERN, Dubna, Edinburgh, Ferrara, Mainz, Orsay, Perugia, Pisa, Saclay, Siegen, Torino, Vienna). We thank our colleagues for their stimulation and support and, in particular, H. Blümer and C. Ebersberger for permission to reproduce the data of Figure 12.

¹¹ In fact, simulation, using the programme 'HALO' [19], has shown that a dipole magnet of the same bending power (14.4 T.m) in place of the bent crystal would lead to a ten-fold increase in the flux of background muons through the NA48 detectors.

8. REFERENCES

- [1] G.D. Barr et al., NA48 Collaboration, "Proposal for a Precision Measurement of ϵ'/ϵ in CP-violating $K^0 \rightarrow 2\pi$ Decays", CERN/SPSC/90-22/P253, 20th July 1990.
- [2] J. Lindhard, Kgl. Danske Videnskab. Selskab, Mat. Fys. Medd. 34 (1965) No.14; Phys. Lett. 12 (1964) 126.
- [3] E.N. Tsyganov, Fermilab TM-682, TM-684, Batavia, 1976.
- [4] A.H. Sørensen and E. Uggerhøj, Nucl. Sci. Appl. 3 (1989) 147.
- [5] J.S. Forster et al., Nucl. Phys. B 318 (1989) 301.
- [6] S.P. Møller, "Crystal Channeling or How to build a '1000 Tesla Magnet'", CERN 94-05, 13th October 1994.
- [7] A.F. Elishev et al., Phys. Lett. 88 B (1979) 387.
- [8] J.F. Bak et al., Phys. Lett. B 93 (1980) 505; Nucl. Phys. B 242 (1984) 1.
- [9] S.I. Baker et al., Nucl. Instr. and Meth., A 234 (1985) 602.
- [10] M.D. Bavizhev et al., "70 GeV Proton Beam Splitting with a Bent Single Crystal", IHEP 89-77, Serpukhov, 1989.
- [11] S.P. Møller et al., Phys. Lett. B 256, 1 (1991) 91.
- [12] B.N. Jensen et al., Nucl. Instr. and Meth. B 71 (1992) 155.
- [13] S.P. Møller et al., Nucl. Instr. and Meth. B 84 (1994) 434.
- [14] P. Grafström et al., Nucl. Instr. and Meth. A 344 (1994) 487.
- [15] S.I. Baker et al., Nucl. Instr. and Meth. B90 (1994) 119.
- [16] K.L. Brown and Ch. Iselin, "DECAY TURTLE - A Computer Program for Simulating Charged Particle Beam Transport Systems, including Decay Calculations", CERN 74-2, 5th February 1974.

- [17] M. Clément, N. Doble, L. Gatignon and P. Grafström, "Tests of Proton Channeling in Bent Crystals with a View to a Future Beam Line Application", CERN/SL 92-21 (EA), NA48 Note 92-5, 21st April 1992.
- [18] H. Blümer and C. Ebersberger, "A Scintillating Fiber Proton Beam Profile Monitor", submitted to Nucl. Instr. and Meth. A (1995).
- [19] Ch. Iselin, "HALO - A Computer Program to Calculate Muon Halo", CERN 74-11, 29th August 1974.

TABLE I GEOMETRICAL PARAMETERS OF THE BENT CRYSTAL

Parameter	Symbol : Formula	Design value
Crystal length	L	60.0 mm
width	w	18.0 mm
thickness	t	1.5 mm
Length of bent part	$D =$ Distance between rollers (Fig.2)	56.0 mm
Bending radius	R	3.0 m
Crystal bend angle	$\theta_o = D/R$	18.67 mrad
Minimum force per roller to bend the crystal	$T_{\min} = \theta_o 10^{-3} \frac{E w t^3}{3 D^2}$	≈ 1.6 kg
Young's modulus (Si)	E	$\approx 1.3 \cdot 10^4$ kg/mm ²
Required beam deflection angle	$\theta = \frac{l}{D} \theta_o \cos \varphi$ $= \frac{w}{R} (\frac{1}{\sin \varphi} - \sin \varphi)$	9.6 mrad
Horizontal angle of rotation	$\varphi = \pm \arcsin \left[\sqrt{a^2 + 1} - a \right]$ $a = R \frac{\theta}{2w}$	$\pm 28.73^\circ$ 0.80
Vertical angle of inclination	$\alpha = \frac{\theta}{2 \cos \varphi}$	+ 5.5 mrad
Length of crystal used by beam	$l = \frac{w}{\tan \varphi}$	32.8 mm
Effective length traversed	$l_{\text{eff}} = \frac{l}{\cos \varphi} = \frac{w}{\sin \varphi}$	37.5 mm
Effective bending radius for beam	$R_{\text{eff}} = \frac{R}{\cos \varphi}$	3.42 m
Beam deflection sensitivity to φ	$\frac{\Delta \theta}{\Delta \varphi} = - \frac{w}{R} \cos \varphi \left(\frac{1}{\sin^2 \varphi} + 1 \right)$	-0.28 mr/mr = -0.49 mr/ $^\circ$
Coupling: beam vertical angle / horizontal position	$\frac{\Delta y'}{\Delta x} = \frac{1}{R \tan \varphi}$.61 mrad/mm
Crystal vertical angle /horizontal position	$\frac{\Delta \alpha}{\Delta x} = - \frac{1}{R} \sin \varphi$	-0.69 mrad/mm

TABLE II CHANNELING PROPERTIES OF THE SILICON CRYSTAL

Property	Symbol : Formula	Value
Proton beam momentum	p	450 GeV/c
Critical angle for channeling w.r.t. Si (110) planes [6]	$\Psi \approx \frac{140}{(\mu rad)} \cdot p^{-1/2}$	$\approx 7 \mu rad$
Dechanneling length in straight crystal [6]	$l_o \approx \frac{0.8}{(mm)} \cdot p$	$\approx 350 \text{ mm}$
Dechanneling length in bent crystal [6]	$l_o^* = l_o (1 - F)^2$	$\approx 56 \text{ mm}$
Critical radius for channeling [3]	$R_c \approx \frac{8 \cdot 10^{-4}}{(m)} \cdot p$	$\approx 0.37 \text{ m}$
Curvature in units of R_c^{-1}	$\Gamma = R_c/R_{eff} \approx \frac{p}{1220 \cdot R_{eff}}$	≈ 0.11
Dechanneling parameter due to bending [5]	$F \approx 1.04 \tanh 6\Gamma$ ¹²⁾	≈ 0.6
Surface transmission for beam within angle $\pm\Psi$ w.r.t. Si (110) planes [6]	S	≈ 0.7
Transmission factor through crystal	$\eta = (1 - F) e^{-\frac{l_{eff}}{l_o^*}}$	≈ 0.20
Overall transmission within crystal acceptance	$S \cdot \eta$	≈ 0.14
Effective bending power of crystal	$B^* \cdot l_{eff} = \frac{\theta}{(mrad)} \cdot \frac{p}{299.8}$	$\approx 14.4 \text{ Tm}$
Equivalent magnetic field (compare [6])	B^*	$\approx 384 \text{ Tesla}$

¹²⁾ Empirical formula fitting the theoretical curve of reference [5]

TABLE III COMPARISON OF NOMINAL AND TUNED CRYSTAL SETTINGS

Co-ordinate	Nominal Settings	Tuned Settings =		Centre	Tuned	
				Off-Set	±	Values
Horizontal Angle, ϕ°	+ 28.7°	+ 30.1°	- 28.1°	+ 1.0	±	29.1°
Vertical Angle, α (mrad)	+ 5.5	+ 4.7	+ 4.1	- 1.1	±	0.3
Horizontal Displ., x (mm)	0.0	0.0	0.0	0.0	±	0.0
Vertical Displ., y (mm)	0.0	- 1.5	- 1.3	- 1.4	m	0.1

TABLE IV TUNED SETTINGS FOR SECOND CRYSTAL

Co-ordinate	Tuned Settings =		Centre	Tuned	
			Off-Set	±	Values
ϕ°	+ 29.1°	- 27.5°	+ 0.8	±	28.3°
α (mrad)	+ 4.3	+ 3.9	- 1.4	±	0.2
x (mm)	- 1.0	- 1.0	- 1.0	±	0.0
y (mm)	- 1.1	- 1.1	- 1.1	±	0.0

Figure Captions

- Figure 1 Schematic Layout of Simultaneous K_L and K_S Beams (Vertical Section).
- Figure 2 Co-ordinate System and Geometry of the Bent Crystal.
- Figure 3 Phase-space Diagrams for the Propagation of the Proton Beam from the K_L TARGET to the CRYSTAL and thence to the TAGGER (in the Vertical (y, y') and Horizontal (x, x') Planes).
- Figure 4 Mechanical Design of the Crystal Holder and Bending Device.
- Figure 5 Photographs of the Crystal Holder and Goniometer.
- Figure 6 Successive Tuning Scans of the Relative Proton Beam Flux onto the TRIG counter (Figure 1) as Functions of Crystal Goniometer Settings (for $\varphi \sim +30^\circ$):
- a) Vertical Rotation Angle, α ;
 - b) Horizontal Rotation Angle, φ ;
 - c) Vertical Rotation Angle, α ;
 - d) Vertical Displacement, y;
 - e) Horizontal Rotation Angle, φ .
- Figure 7 Horizontal and Vertical Profiles of the Proton Beam selected by the Crystal and transmitted onto the Wire Chamber, MWPC (Figure 1); (with crystal settings : $\varphi = +30.1^\circ = +4.7 \text{ mrad}$, $x = 0.0 \text{ mm}$, $y = -1.5 \text{ mm}$).
- Figure 8 Tuning Scans as Functions of Crystal Goniometer Settings (for $\varphi \sim -30^\circ$):
- a) Vertical Rotation Angle, α ;
 - b) Vertical Displacement, y;
 - c) Horizontal Rotation Angle, φ .
- Figure 9 Scan of the Relative Proton Beam Flux onto the TAGGER as a Function of the Current in a Horizontal Steering Magnet, TRIM 5, (located at an intermediate beam focus upstream of the K_L target); (with crystal settings as for Figure 7).

- Figure 10 Horizontal and Vertical Profiles of the Proton Beam onto MWPC, for :
- a) TRIM 5 Current = -22 A (Setting P in Figure 9), corresponding to maximum proton transmission to the K Σ target;
 - b) TRIM 5 Current = -12 A (Setting Q in Figure 9), corresponding to nominal proton transmission to the K Σ target.
- Figure 11 Horizontal and Vertical Profiles of the Proton Beam onto MWPC, obtained with the Second Crystal (for TRIM 5 current = -22 A and crystal settings :
 $\varphi = -27.5^\circ$, $\alpha = +3.9$ mrad, $x = -1.0$ mm, $y = -1.1$ mm).
- Figure 12 Horizontal and Vertical Profiles of the Proton Beam onto a Hodoscope at the TAGGER, obtained with the Second Crystal (for TRIM 5 current = -12 A and crystal settings as for Figure 11).

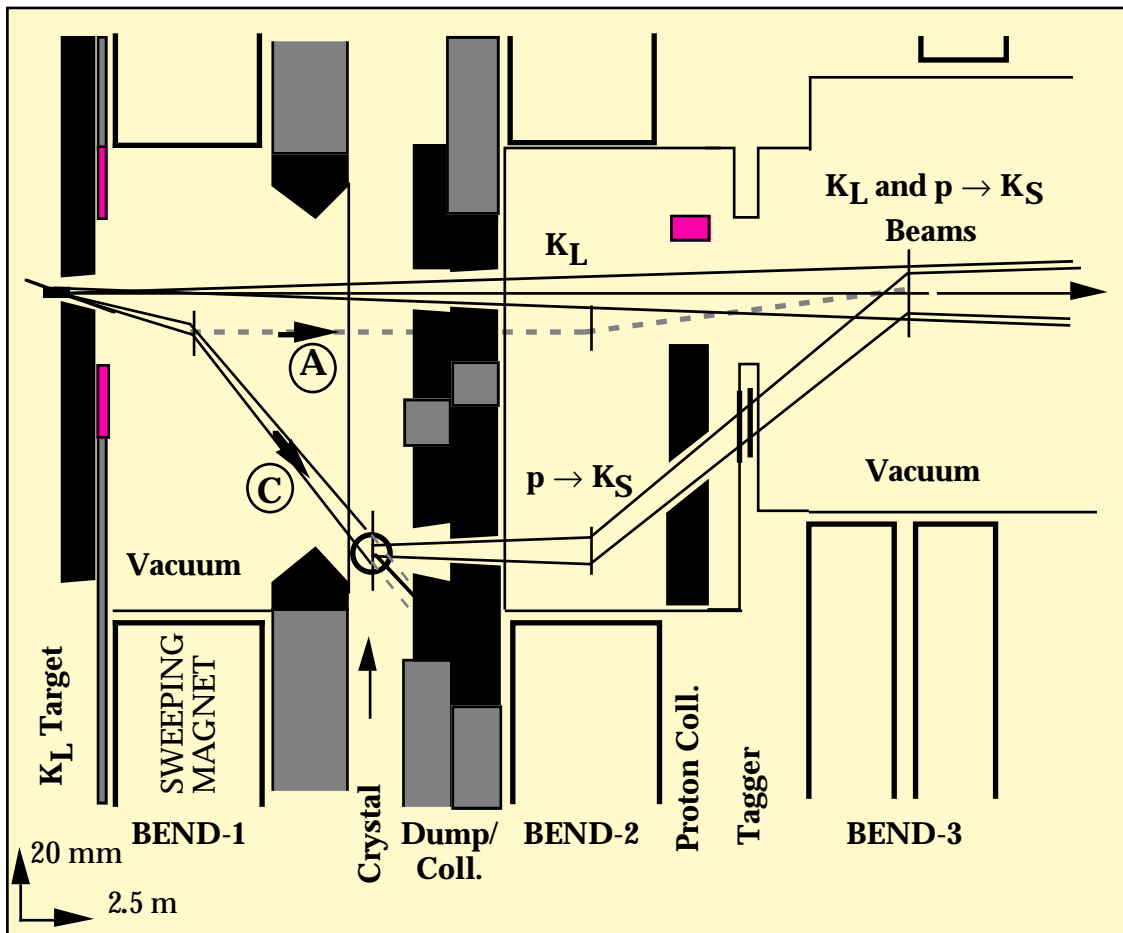
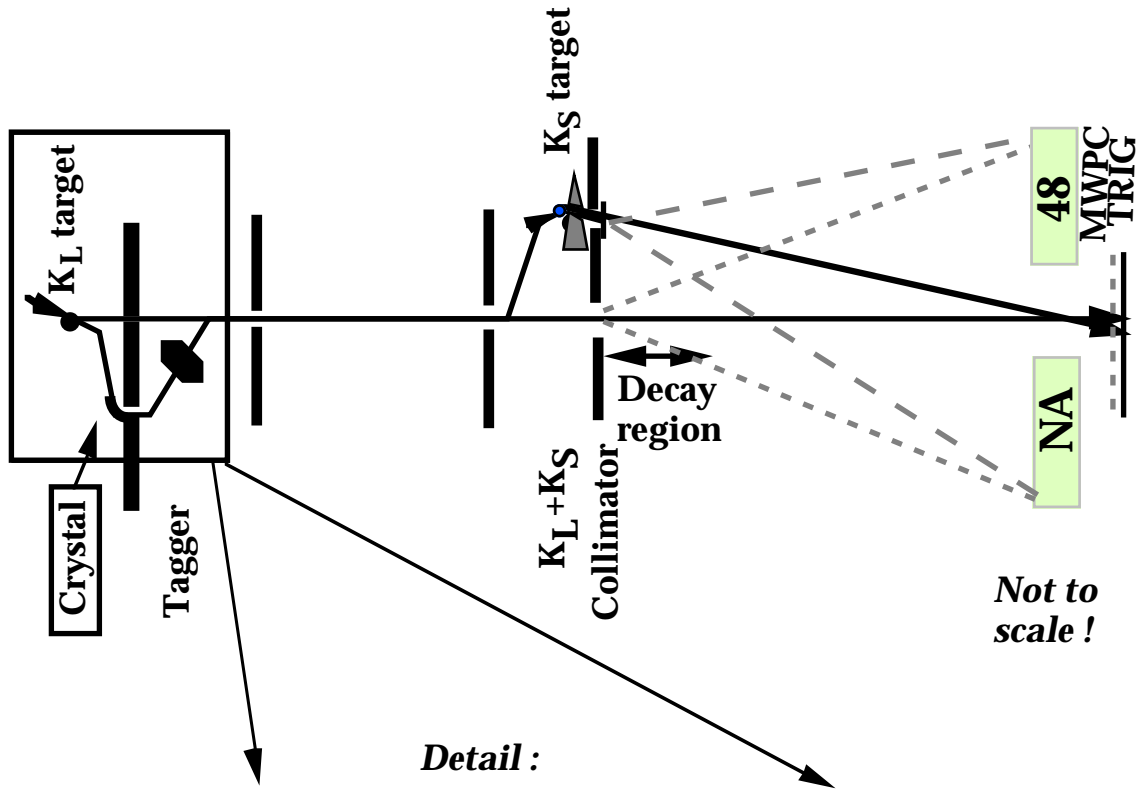
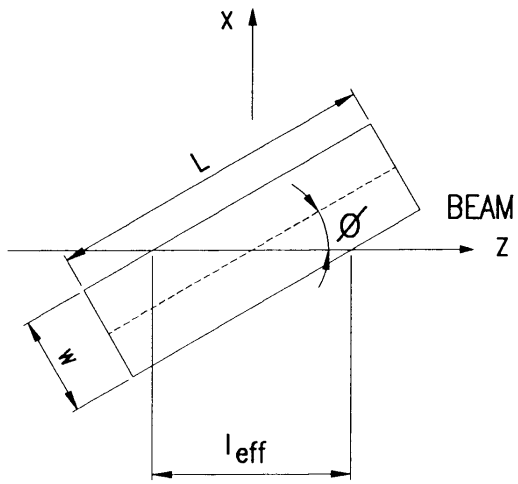
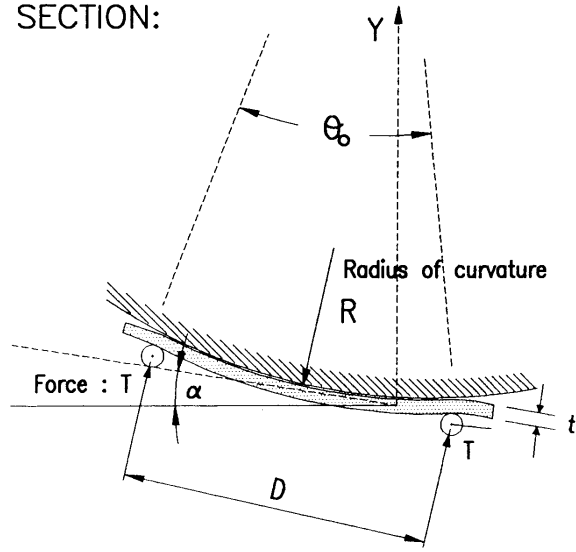


Figure 1

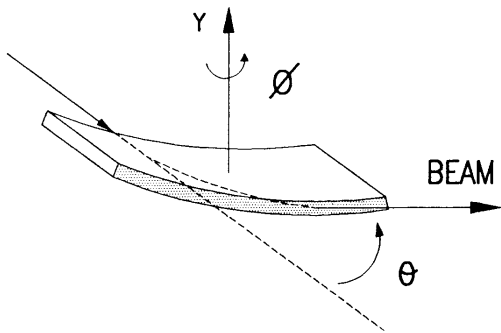
PLAN:



VERTICAL SECTION:



SIDE PERSPECTIVE:



AS SEEN BY BEAM:

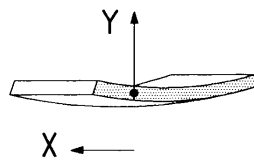
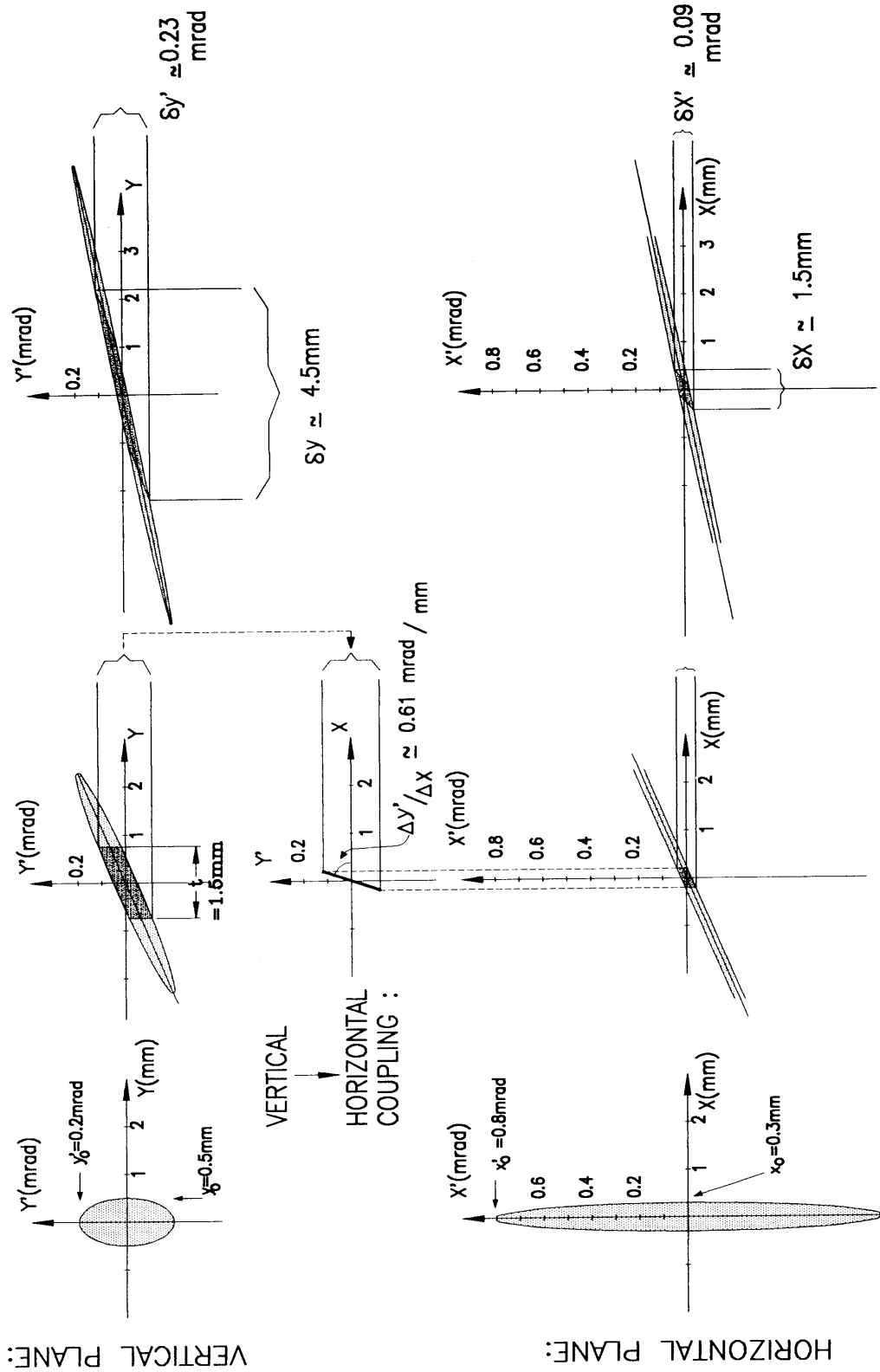


Figure 2



K_L TARGET ($Z=0$) → CRYSTAL ($Z=10.95m$) → TAGGER ($Z=23.9m$) Figure 3

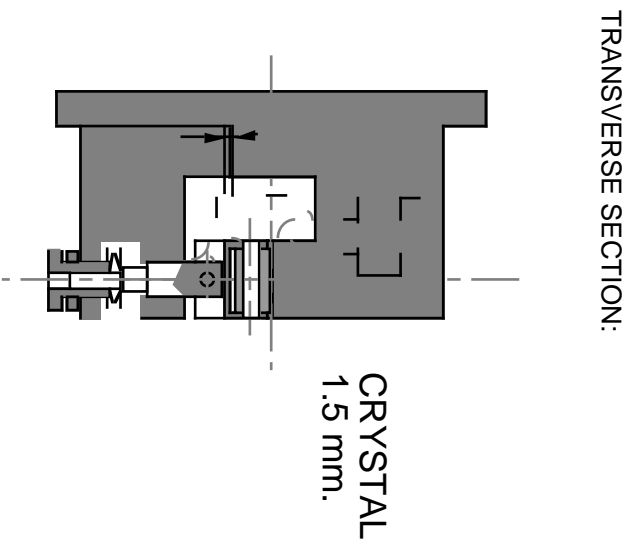
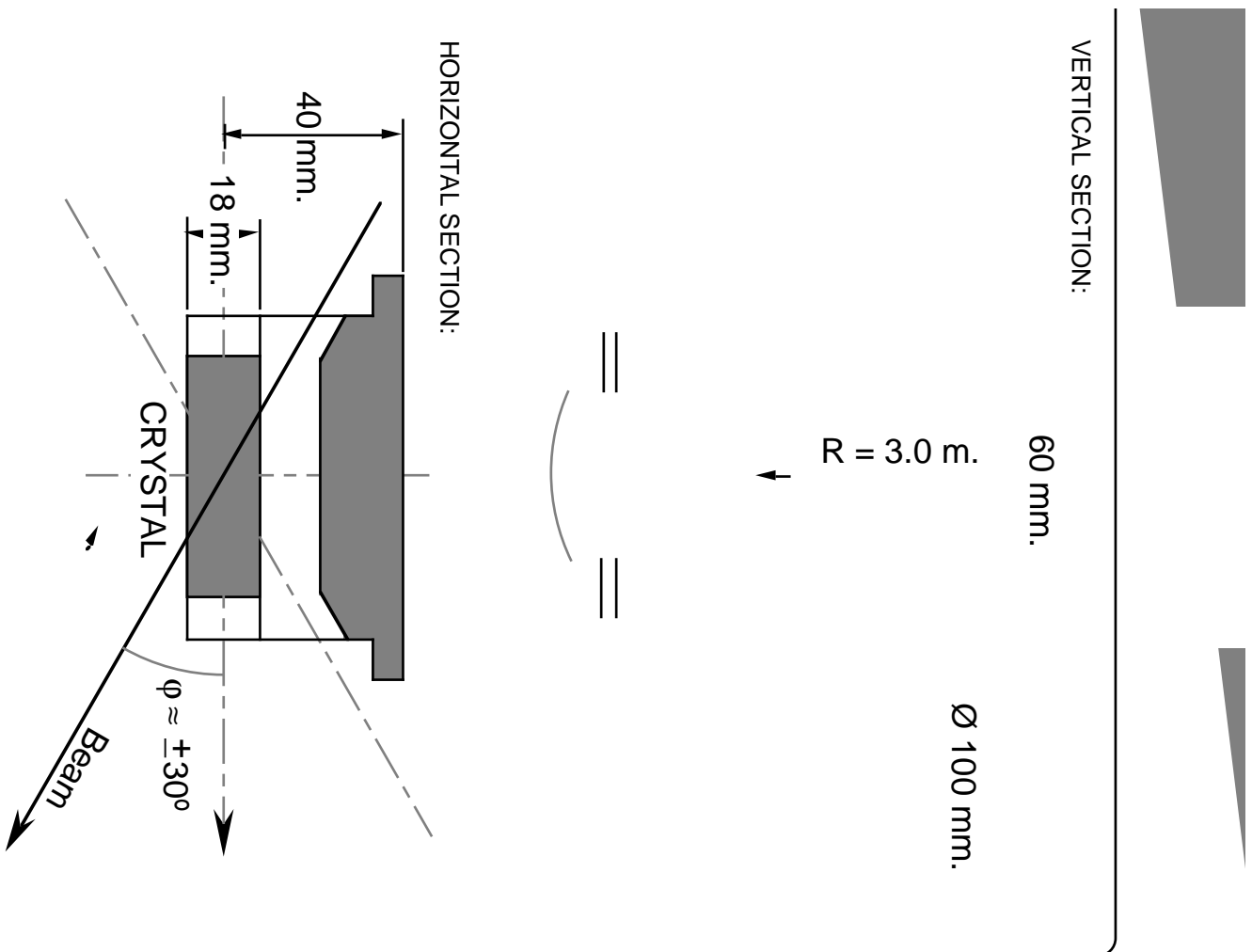


Figure 4

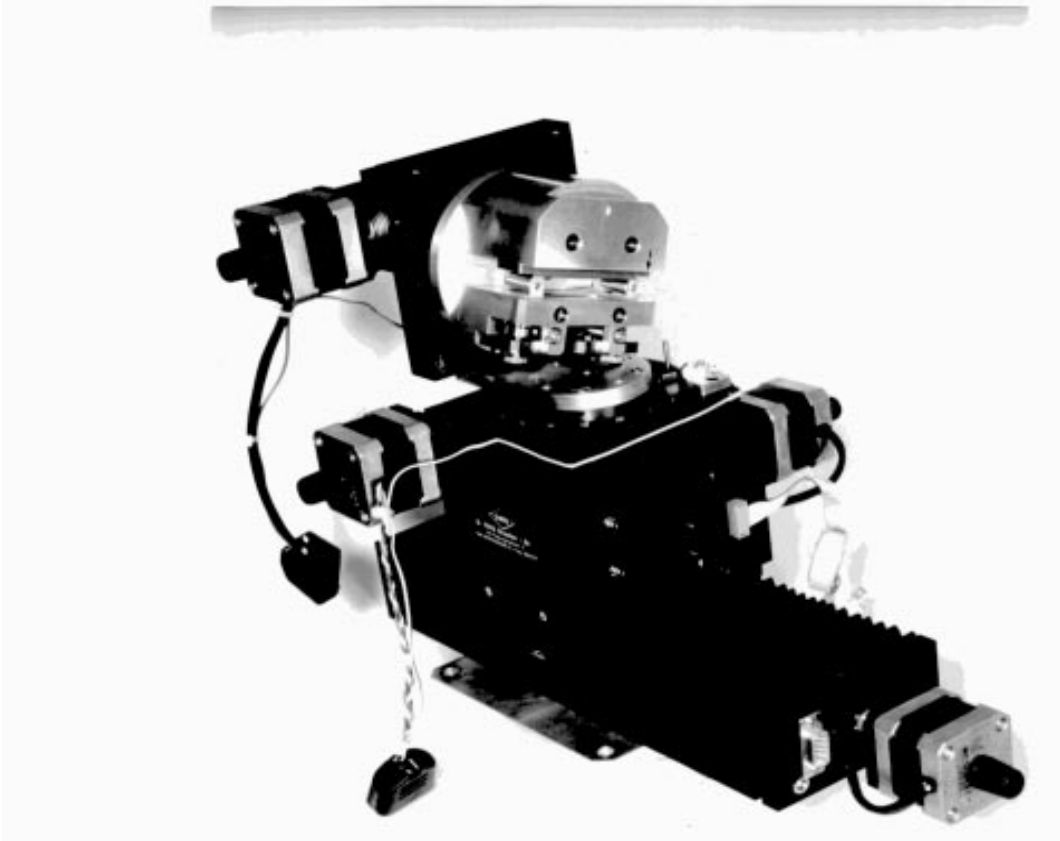
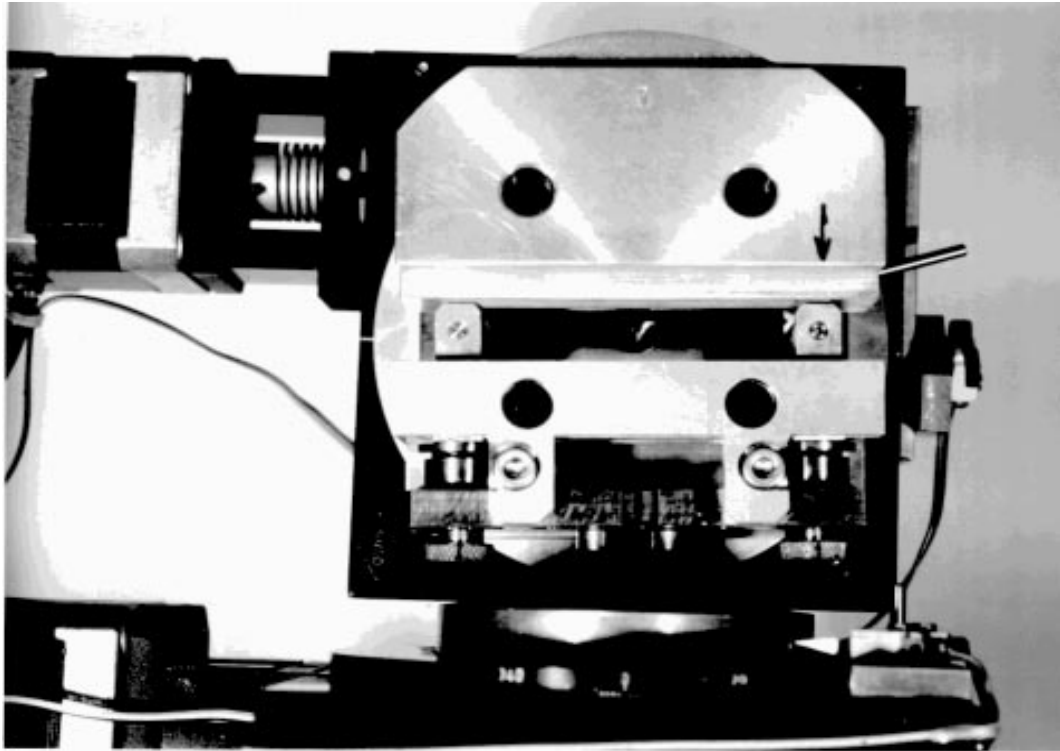


Figure 5

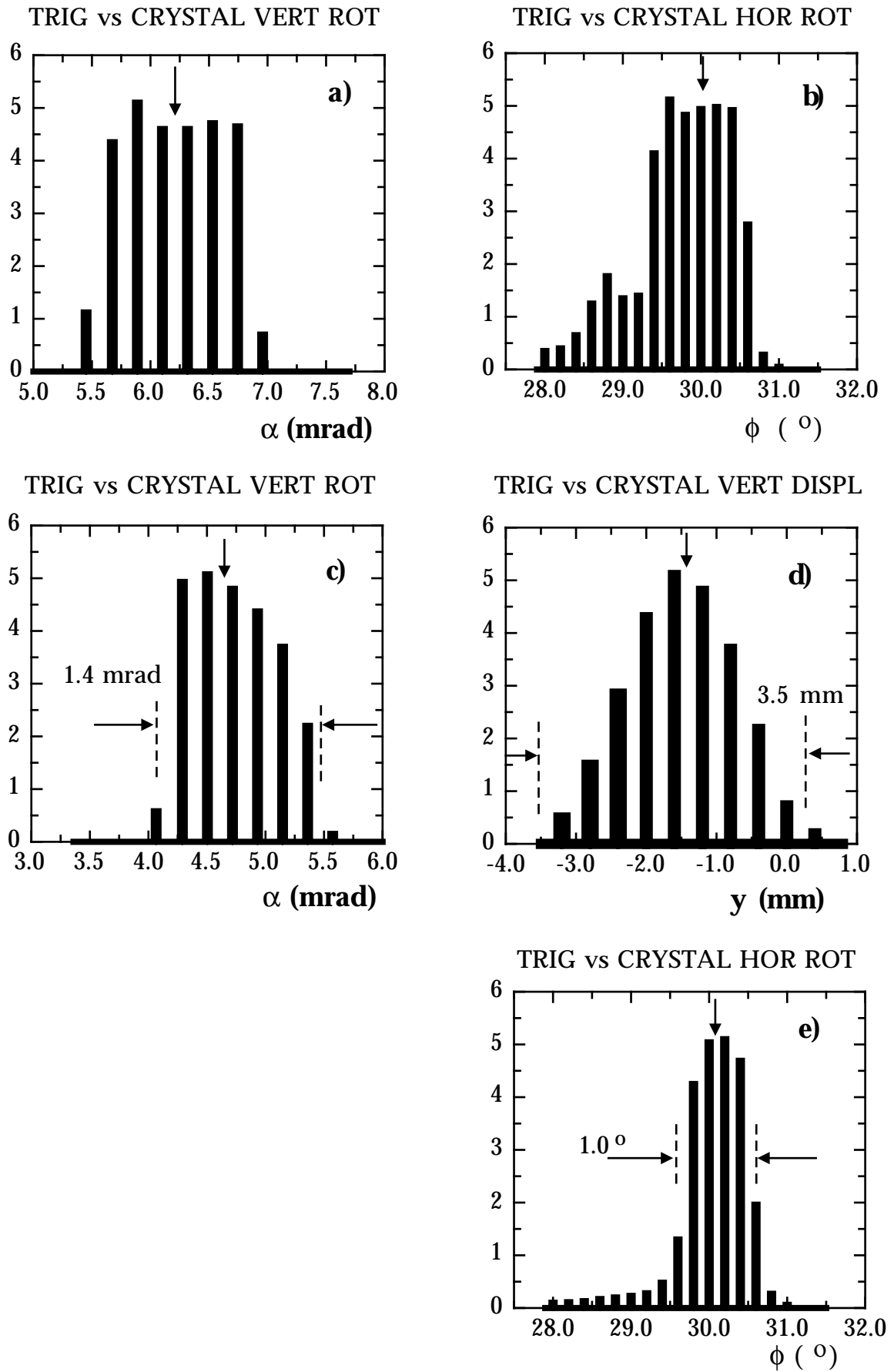
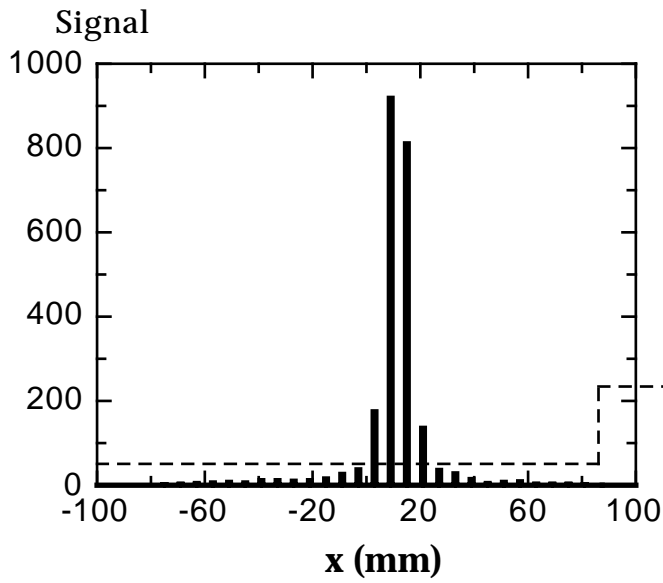


Figure 6

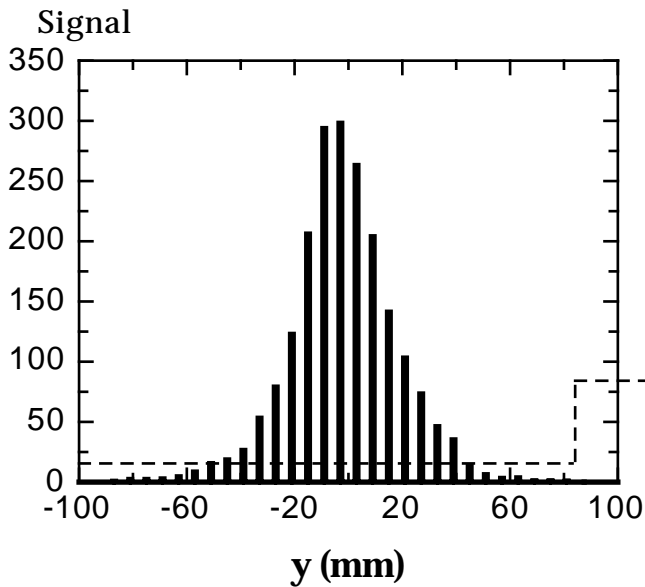
MWPC HORIZONTAL



Wire spacing : 6 mm
High Voltage : 2220 V

5% cut values :
Average = 11.6 mm
R.M.S. = 4.5 mm

MWPC VERTICAL



Wire spacing : 6 mm
High Voltage : 2220 V

5% cut values :
Average = 3.0 mm
R.M.S. = 18.1 mm

Figure 7

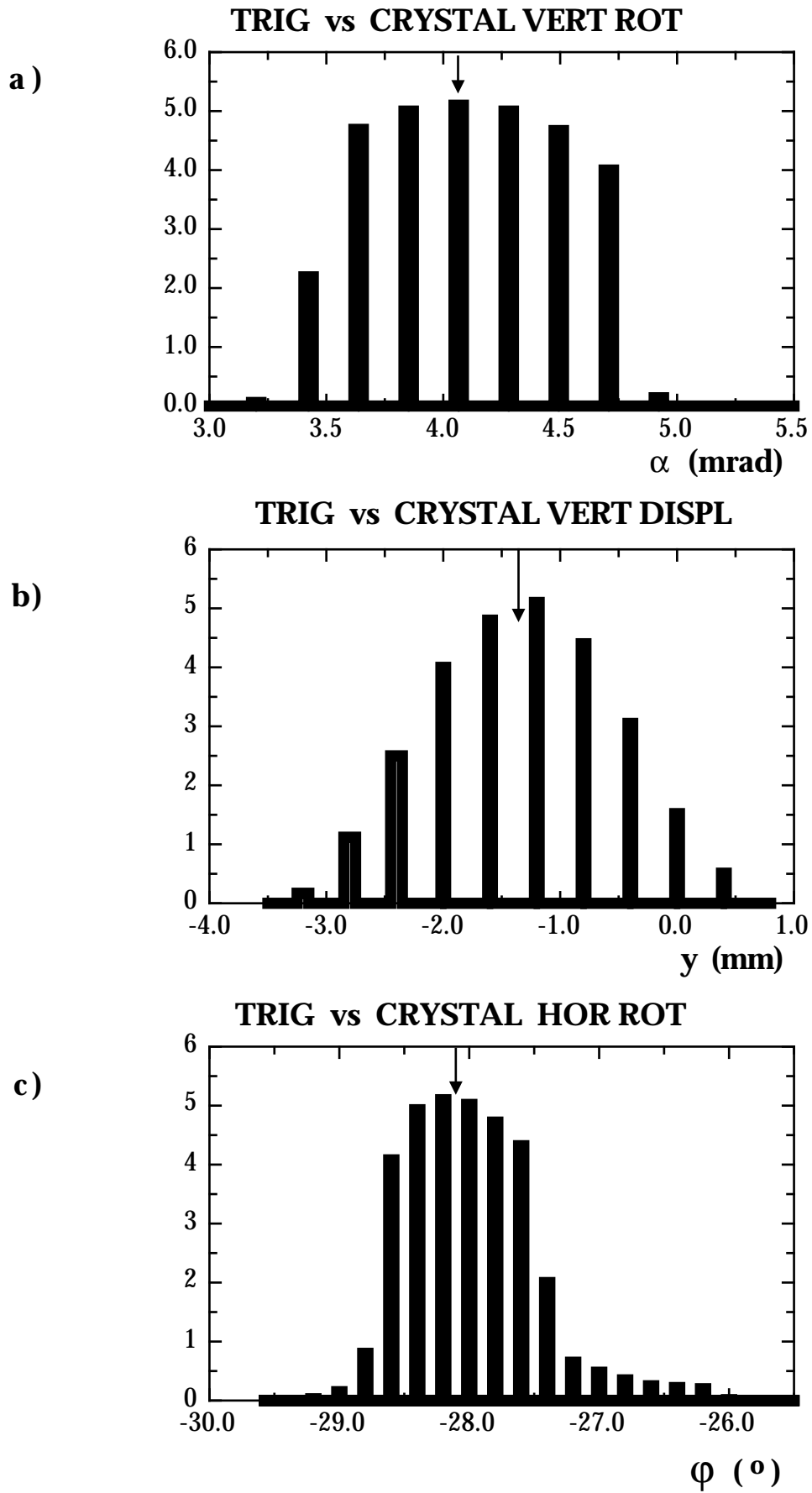


Figure 8

TAGGER vs TRIM-5

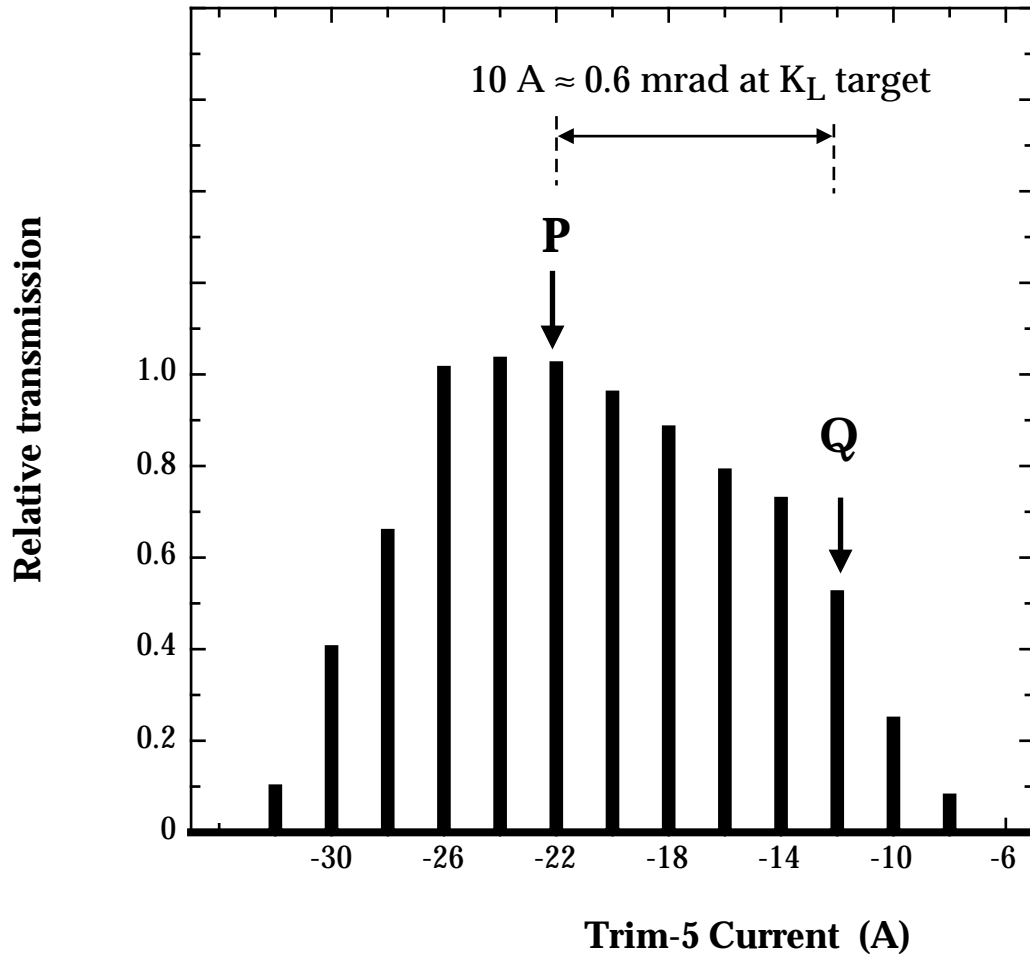
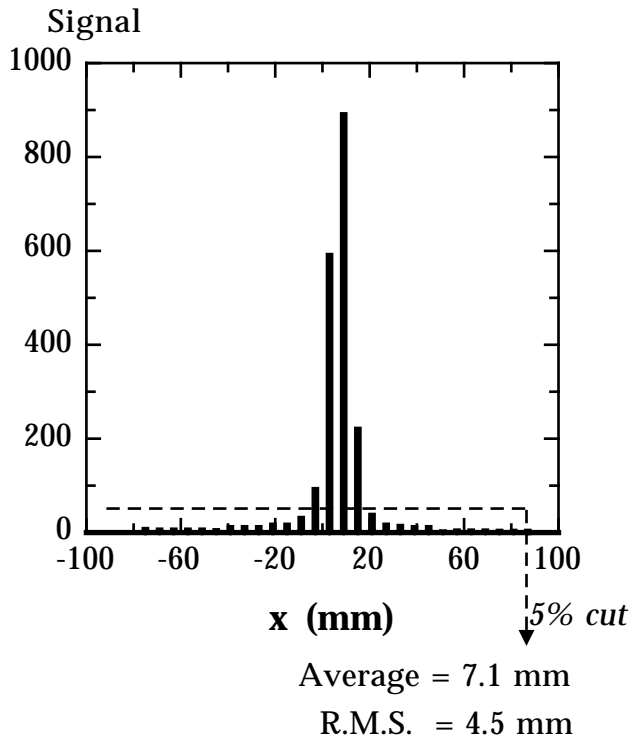
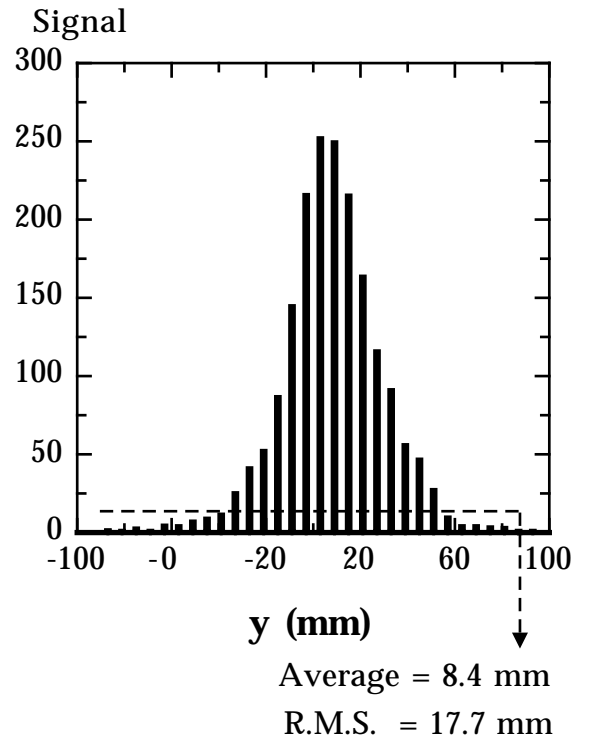


Figure 9

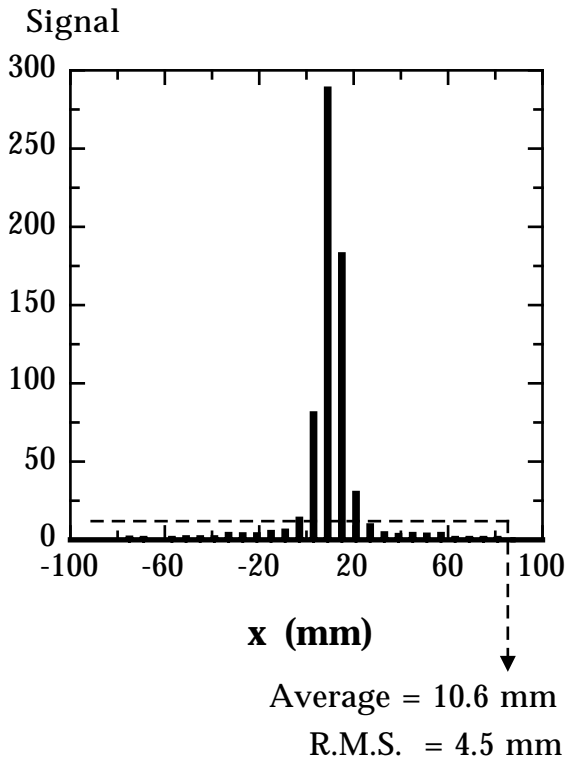
a) MWPC HORIZONTAL



MWPC VERTICAL



b) MWPC HORIZONTAL



MWPC VERTICAL

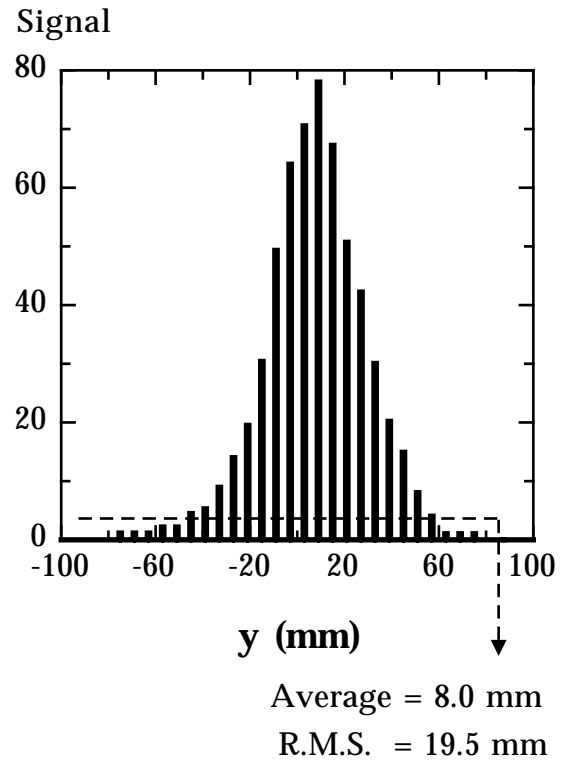
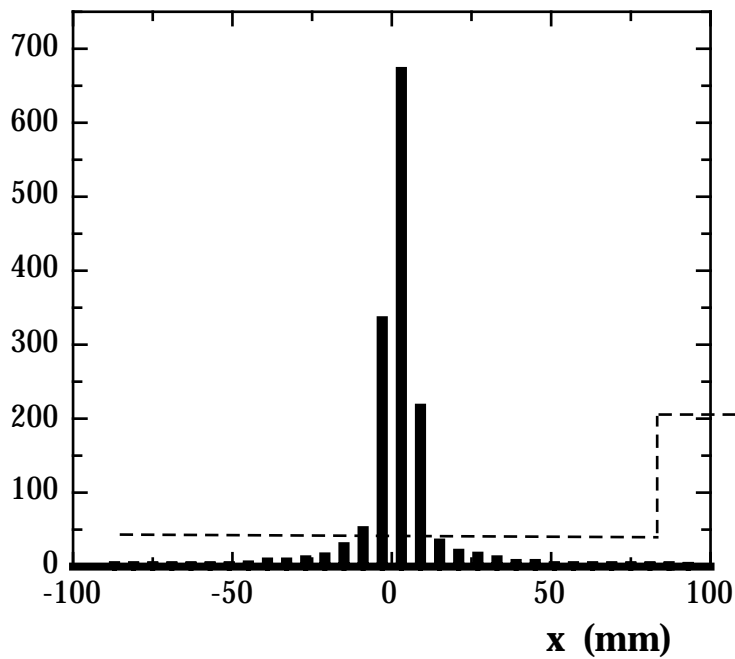


Figure 10

MWPC HORIZONTAL

Signal



Wire spacing : 6 mm

High Voltage : 1980 V

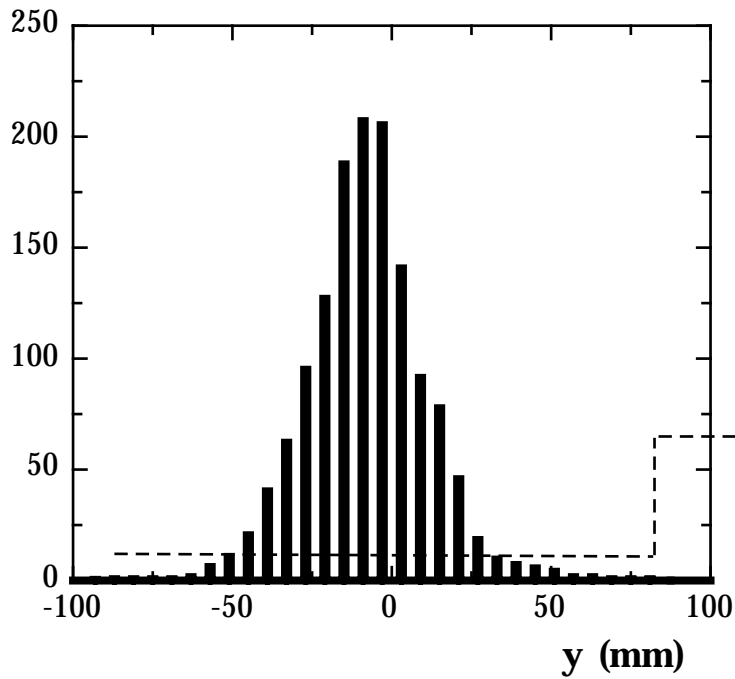
5% cut values :

Average : 2.0 mm

R.M.S. : 4.5 mm

MWPC VERTICAL

Signal



Wire spacing : 6 mm

High Voltage : 1980 V

5% cut values :

Average : -8.5 mm

R.M.S. : 15.6 mm

Figure 11

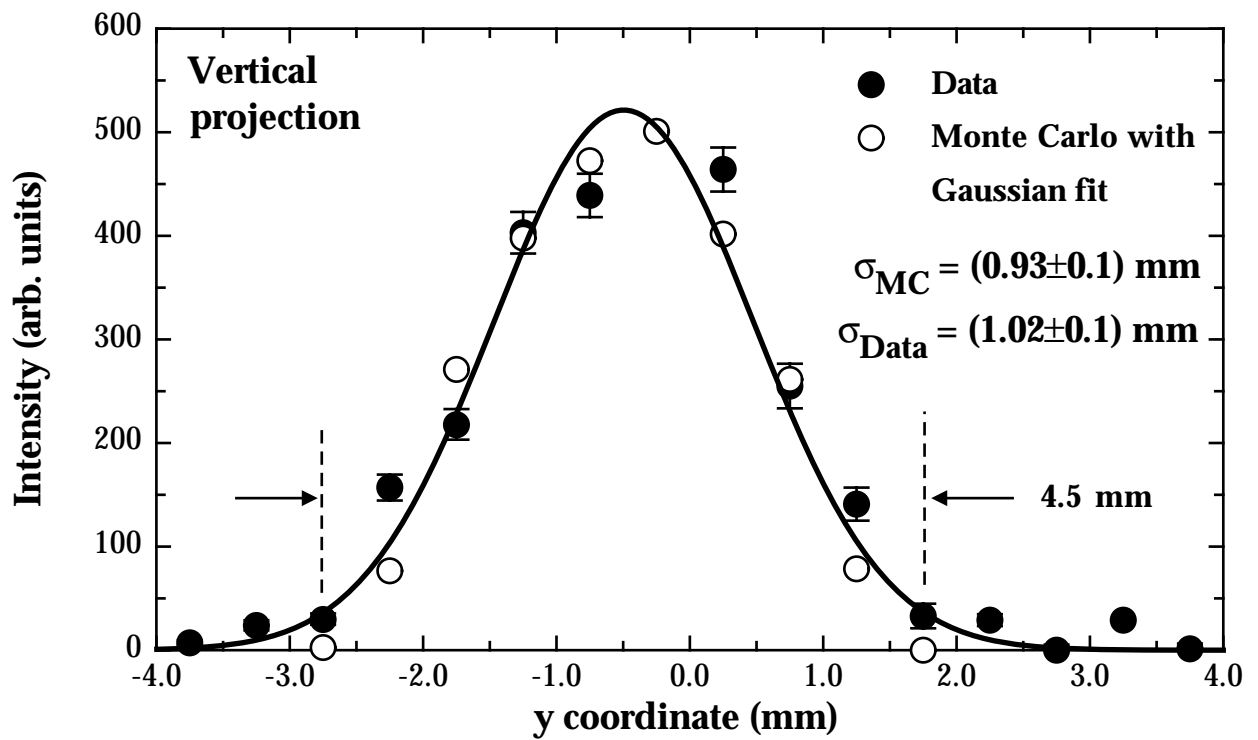
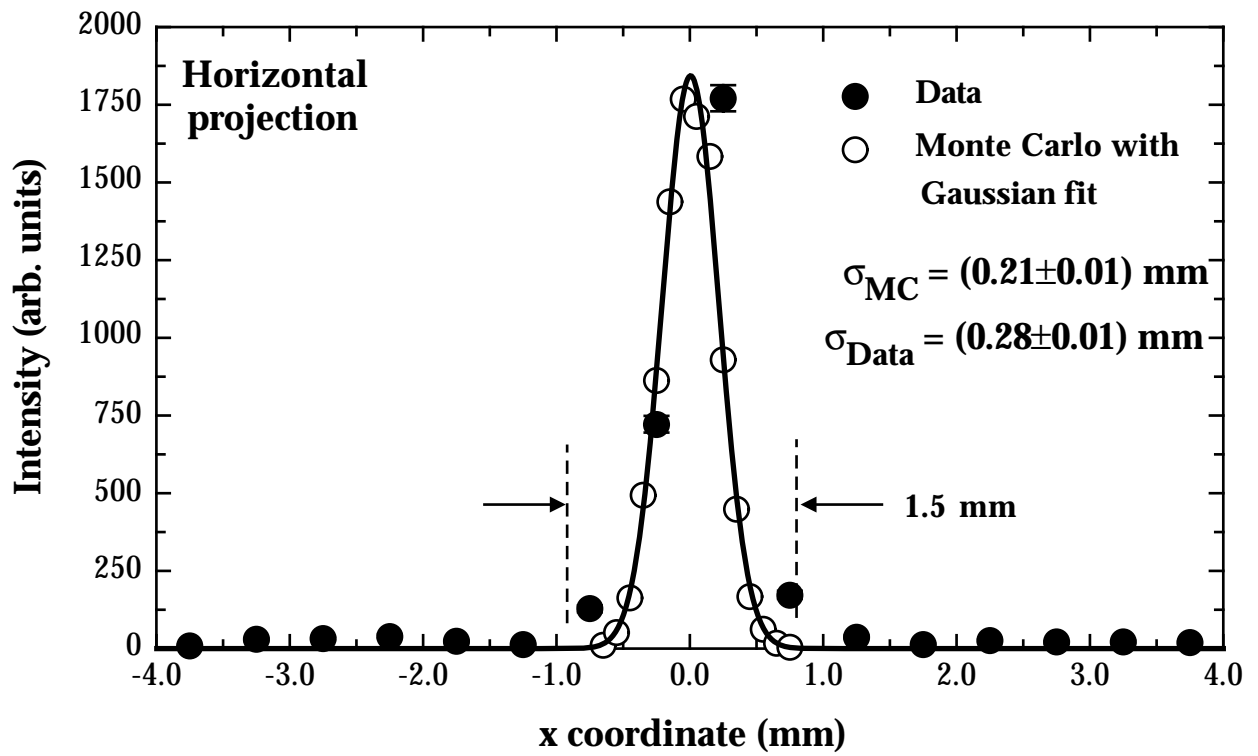


Figure 12